Decoupling of functional traits from intraspecific patterns of growth and drought stress resistance

Kelly L. Kerr[1*], Jaycie C. Fickle[1], William R.L. Anderegg[1, 2]

[1]School of Biological Sciences, University of Utah, Salt Lake City, UT 84112, USA

[2]Wilkes Center for Climate Science and Policy, University of Utah, Salt Lake City, UT 84112, USA

*Author for correspondence:

Kelly Kerr

Address: 257 S 1400 E Room 210, Salt Lake City, UT 84112

Telephone: +1-925-360-8594

E-mail: kellykerr@ucsb.edu

	Word count		
Total for main text	7,936	No. of figures	7 (all in color)
Summary	199	No. of tables	0
Introduction	881	No. of supporting information files	1 (Tables S1-S6; Figs. S1-S9)
Materials and Methods	3,066		
Results	823		
Discussion	2,166		

Summary

- Intraspecific variation in functional traits may mediate tree species' drought resistance, yet it remains unknown if trait variation is due to genotype (G), environment (E), or GxE interactions. Understanding the drivers of intraspecific trait variation and whether variation mediates drought response can improve predictions of species' response to future drought.
- Using populations of quaking aspen spanning a climate gradient, we investigated intraspecific variation in functional traits in the field as well as the influence of G and E among propagules in a common garden. We also tested for trait-mediated trade-offs in growth and drought stress tolerance.

- We observed intraspecific trait variation among the populations, yet this variation did not necessarily translate to higher drought stress tolerance in hotter/drier populations. Additionally, plasticity in the common garden was low, especially in propagules derived from the hottest/driest population. We found no growth-drought stress tolerance trade-offs and few traits exhibited significant relationships with mortality in the natural populations, suggesting that intraspecific trait variation among the traits measured did not strongly mediate responses to drought stress.
- Our results highlight the limits of trait-mediated responses to drought stress and the complex GxE interactions that may underly drought stress tolerance variation in forests in dry environments.

Keywords: local adaptation, phenotypic plasticity, genotype, environment, climate change, drought tolerance, aspen, *Populus tremuloides*

Introduction

Current research suggests there will likely be a mismatch between the rate of climate change and the ability of certain forest tree species to acclimate, either in-place or by migration (Aitken et al. 2008). Acclimation via phenotypic plasticity, the altering of phenotypes in response to environmental change, will be critical for many species (Bradshaw 1965, Franks et al. 2014), particularly in the absence of somatic mutations that can result in phenotypic change in long-lived organisms (Whitham and Slobodchikoff 1981) and when migration is not a viable option (Jump and Peñuelas 2005). Major environmental changes currently threatening tree species worldwide include more severe and frequent drought events (Dai 2013), which may result in increased widespread mortality of critical forest ecosystems (Allen et al. 2015). It is thus crucial to understand which species and/or populations in drought-prone regions will be able to acclimate to drought stress to improve predictions of species' response to future drought as well as management and conservation efforts (Sperry et al. 2019, Trugman et al. 2021).

Several plant phenological responses as well as morphological and physiological functional traits are expressed through genetic control, environmental cues, or an interaction of genetics and environment that underlie species' drought stress response (Nicotra et al. 2010). Determining the extent to which drought stress response is the result of genotype (G, local

adaptation), environment (E, phenotypic plasticity), or genotype by environment (GxE) interactions is necessary to improve understanding of species' acclimation potential. If populations from cooler/wetter climates are locally adapted to current environments they may suffer under future drought due to maladaptation to low water availability, while populations with phenotypic plasticity will have a greater capacity to acclimate to drought (Aitken et al. 2008). Provenance trials and common garden studies that compare distinct populations under controlled environmental conditions provide valuable insight into genotype and environmental influence on phenology and functional traits. While most common garden studies focus on plant phenology and growth, some have investigated functional traits related to drought stress resistance, such as leaf area-to-sapwood area ratios and xylem vulnerability to cavitation. These studies have shown both low (Kavanagh et al. 1999, Lamy et al. 2014, Kerr et al. 2015, Varone et al. 2016) and high phenotypic plasticity (Maherali et al. 2002, St. Clair et al. 2010, Blackman et al. 2017, Pritzkow et al. 2020), as well as GxE interactions (López et al. 2013) in functional traits.

For long-lived organisms like trees, classic ecological theory suggests that growth-stress tolerance trade-offs are expected to underlie intraspecific variation in functional traits (Grime 1977, Adler et al. 2014, Reich 2014). A growth-stress tolerance trade-off suggests that under harsh environment conditions, tree species/populations will exhibit a trade-off by constraining growth for improved stress tolerance. There are a variety of functional traits (drought resistance traits) that allow individuals to tolerate periods of low water availability. Trees with improved drought resistance may have xylem more resistant to drought-induced cavitation (Tyree and Sperry 1989, Maherali et al. 2004), denser leaves with less water demand and more tolerance of increased xylem pressure during drought (Wright *et al.* 2004), lower leaf area-to-sapwood area ratios which reduces evaporative demand and the xylem pressure required to move water to the foliage (Martínez-Vilalta *et al.* 2009), increased production of root tissue and deeper roots for more efficient uptake of water from soil (Jackson et al. 2000), and leaves with lower turgor loss points (Bartlett et al. 2014) and higher heat tolerance (Knight and Ackerly 2002). Given the carbon costs associated with these traits, trees with tolerance to drought might be expected to grow slower under wetter conditions to survive drier climate conditions. A more thorough understanding of which functional traits mediate growth-stress tolerance trade-offs will improve our predictions of species' drought response.

Here, we examined within-species variation in growth, drought resistance traits, and growth-stress tolerance trade-offs among populations of quaking aspen (aspen, *Populus tremuloides*), a widespread, foundational tree species in North America and the Intermountain West of the United States (McAvoy et al. 2012). While clonality is a common phenomenon in this species, aspen genetic diversity in the Intermountain West can be high with landscapes composed of numerous, spatially clustered, unrelated genets (Mock et al. 2008). In recent decades, aspen in the region have experienced extensive drought-induced mortality events (Worrall et al. 2008, Anderegg et al. 2012). Given the threat of future droughts of increased frequency and severity, it is vital to improve our understanding of the acclimation potential of aspen to better manage these forests. Using both natural populations of aspen along an aridity gradient and an associated common garden experiment, we aimed to answer the following questions: Q1) Among natural populations, do genetically distinct aspen exhibit drought resistance trait variation reflective of local climate?; Q2) In a common garden, do aspen propagules exhibit drought resistance trait variation whereby: a) propagules that originate from hotter/drier climates exhibit higher drought resistance (G effects); b) all propagules, regardless of climate of origin, respond similarly to differing drought conditions (E effects); or c) response to drought conditions is dependent on the genotype of the propagule (GxE interactions)?; Q3) In a common garden, is there a trait-mediated trade-off between growth (as measured with relative growth rates) under wet conditions and stress tolerance under drought conditions?; and Q4) Does a growth-stress tolerance trade-off occur in natural populations (with growth measured via basal area index)?

Methods

Natural populations

The United States Forest Service Forest Inventory and Analysis (FIA) database was used to generate a list of natural aspen populations spanning a gradient from cool, wet to hot, dry climates in Colorado and Utah (to minimize latitudinal effects across populations). From this list, five populations were selected from the Dixie, San Juan, Uncompaghre, White River, and Uinta National Forests (Fig. 1a), where mean annual temperature ranges from 2.4 °C to 5 °C and mean annual precipitation ranges from 338 mm to 662 mm (Table S1). To sample the genetic diversity within each population, plots were established in 2019 in 6 genetically distinct clones (see

Population genetics section below). Plots were selected to have similar slopes, aspects, and elevation to limit microclimate differences among the populations, and were established within healthy, mature stands well within the boundaries of each clone (e.g., not at leading/trailing edges). Plot centers were marked with a GPS unit and circular, 18-m radius boundaries were demarcated based on plot center. Within each plot, the diameter at breast height (DBH) was measured on trees with a DBH >3 cm (Table S1). Trees were also visually scored for canopy dieback (i.e., mortality) by estimating the percentage (0-100%) of canopy that was recently dying or dead (i.e., foliage present but brown/black and/or dried in upper, sunlit parts of the canopy). Focal trees were selected for measurements (5 for traits and 15 for tree cores) from representative healthy and mature trees. Fully developed leaves were collected and dried on silica gel for DNA extraction from the 5 trait trees to ensure trees within a clone were genetically identical. Plots were visited from late June to early July of 2020 for most of the data collection to ensure measurements were made during peak water stress prior to summer monsoon rainfall that occurs across most of the populations. We were unable to measure all traits in 2020 due to restrictions from the COVID-19 pandemic and samples for pressure volume curve parameters were collected in July 2021. During 2021, we also visually re-scored all trees for canopy dieback. Because 2020 was a severe drought year (Williams et al. 2022), evaluating canopy dieback in 2021 provided a useful estimate of drought stress tolerance among the natural populations.

Common garden

During 2019, root samples were collected from clones for DNA extraction and for propagation (Luna 2003). One to three root segments of ~25 cm length and ~4 cm diameter were cut from one small/medium tree within each clone. Root segments were wrapped in a wet paper towel, placed in a plastic bag, and stored in a cooler. Fully developed leaves were also collected and dried on silica gel. In the laboratory, root segments were rinsed to remove dirt, washed in a 5% bleach solution to kill bacterial or fungal pathogens, and rinsed again in clean water. A small piece of root cambium was removed from each segment and dried in an oven at 50°C. Cleaned root segments were planted in sand:perlite (1:1) and placed on 23°C warming mats in a mist propagation room. New shoots ~3 cm were removed with a sterilized razor blade, dipped in 0.3% IBA (indole-3-butyric acid) hormone powder (Hormex Rooting Powder #3, CA, USA), planted

in perlite:drielite (1:1), and placed back on 23°C warming mats in the mist propagation room. Once propagules developed root systems they were transplanted into soil (Metro Mix 900, Sungro Horticulture Agawam, MA, USA) and placed in a greenhouse. In May 2020, propagules were transplanted into a common garden on the University of Utah campus. Propagules were randomly planted across 10 beds, resulting in a total of 360 plants at a spacing of 50 cm. All beds received mulch and were weeded regularly. Beds were irrigated to field capacity via sprinkler irrigation throughout the 2020 growing season.

During the 2021 growing season, beds in the common garden were irrigated to field capacity until June 25. Then a drought treatment was implemented by first reducing irrigation to ½ full capacity (targeting a predawn leaf water potential of -1 MPa) on half (5) of the beds which had been randomly selected. Irrigation in these drought beds was further reduced to ¼ full capacity when our target predawn leaf water potential value was not being met (Fig S3). The remaining 5 beds received full irrigation (control) throughout the experiment. The common garden site does not have groundwater excess and typically receives limited summer rainfall, therefore rainout exclosures were not constructed.

Population genetics

From each dried root sample, 10-20 mg of tissue was ground in a Minilys tissue homogenizer (Bertin, France) with ceramic beads, and genomic DNA was extracted using a spin-column protocol (Amici et al. 2019). When the root samples were not successful, the corresponding leaf sample was used instead. Individuals were genotyped, to ensure that clones were genetically distinct, at 8 microsatellite loci (Table S2) using primers developed for aspen (Mock et al. 2012). Dye labeled PCR products were resolved by capillary electrophoresis and alleles were determined using PeakScanner Software (version 2.0, Thermo Fisher Scientific). Both diploid and triploid clones were present in the populations although the majority (83%) of clones were triploid (Mock et al. 2008). Frequencies and identities of alleles present per locus in each clone/population were estimated using the "adegenet" (version 2.1.5) R package (Jombart 2008). Loci were highly polymorphic and there was ~5% missing allele data from unsuccessful PCR experiments. Genotypic variability of allele frequencies in the natural populations was determined with multivariate analyses using Principal Components Analysis (PCA) with the "ade4" (version 1.7.18) package (Thioulouse and Dray 2007). Allele frequencies were

179 standardized and constructed on the two main axes (PC1 and PC2) along with the individual
180 trees measured. Genetic variation (F_{ST}) was determined using the "polysat" (1.7.6) R package
181 (Clark et al. 2011) which specializes in mixed ploidy population genetic analyses. F_{ST} varied
182 from 0.04 to 0.12 (Table S3) with geographic distance a likely driver in F_{ST} determination (Fig.
183 1). A subset of 22 propagules in the common garden were randomly selected to verify the
184 genetic identity of the propagule matched the clone of origin (Table S4).
185

186 *Measurements*

187 Natural populations

188 In 2020, large sun-exposed, south-facing, mid-to-upper canopy branches (diameter 5 - 10
189 cm) were collected midday from focal trees using a 20-gauge shotgun. Branches were placed
190 into plastic bags with the branch break wrapped in a wet paper towel and placed into a cooler. In
191 the laboratory, branches were cut under water using a razor blade to produce sample segments
192 with sapwood diameters of ~5 mm and lengths of ~14 cm to accommodate vessel lengths (mean
193 aspen vessel length is ~2 cm, Sperry et al., 1994). All foliage distal to the basal end of each
194 segment was saved for leaf area determination.

195 One set of branches was used for determining native and maximum conductance using
196 the pressure-flow method (Sperry et al. 1988) with a 2% potassium chloride 0.2 μm filtered
197 solution. After measuring native conductance (k_{nat}), samples underwent overnight vacuum
198 infiltration to remove emboli and maximum conductance (k_{max}) was measured (Anderegg et al.,
199 2013). k_{nat} and k_{max} values were standardized by the sapwood area and length of the segment to
200 give native ($K_{s\text{-}nat}$) and maximum ($K_{s\text{-}max}$) sapwood area-specific conductivity, respectively.
201 Percent loss of conductance (PLC) was quantified using equation 1:

202 $$\text{PLC}\ (\%) = \left(\frac{k_{max} - k_{nat}}{k_{max}}\right) \times 100 \qquad (1)$$

203 A second set of branches was used to examine xylem vulnerability. Five branches from
204 each clone were spun in a centrifuge to generate a cavitation-inducing pressure of -2.5 MPa, a
205 pressure that reflects a ~50% loss of conductivity (P_{50}) in aspen (Anderegg et al. 2013, Love et
206 al. 2019). Conductivity values after the spin are reported as $K_{s\text{-}spin}$. We also used P_{50} from full
207 vulnerability curves to test the accuracy of the single spin method. An extra branch from each
208 clone was used to construct vulnerability curves, and therefore 6 branches were used to

209 determine a population-level P_{50} value. Given multiple personnel, laboratory, and fieldwork
210 restrictions from the COVID-19 pandemic we opted to use $K_{s\text{-}spin}$ measurements as a proxy for
211 P_{50}, but we acknowledge that more branch samples and vulnerability curves would be preferable
212 for obtaining better estimations of xylem cavitation resistance. Vulnerability curves were
213 measured using the centrifuge method (Alder et al. 1997). Branch segments were first flushed of
214 embolism via vacuum infiltration and maximum conductance was measured as described above.
215 Then, cavitation-inducing pressures were introduced within the branch using a centrifuge with
216 conductance being measured between pressure points until PLC ~90%. The "fitplc" (version
217 1.2.3) R package was used to fit vulnerability curves and determine P_{50} using a Weibull curve
218 (Duursma and Choat 2017).
219 A third set of branches were used for pressure-volume (PV) curves. Small aspen twigs
220 (diameter ~ 5-10 mm) with healthy, non-necrotic foliage were excised from branches under
221 water >10 cm distance from the branch break and underwent overnight rehydration. Portions of
222 stem that had been under water during rehydration were removed prior to measurement to
223 minimize impacts of oversaturation on the shape of the PV curve (Parker and Pallardy 1987). As
224 samples dried on the benchtop, water potential (Ψ) and weights to the nearest 0.0001 g were
225 measured periodically using a pressure chamber (PMS Instruments) and mass balance. PV curve
226 parameters (Koide et al. 1989) were determined: leaf turgor loss point (Ψ_{TLP}), leaf water
227 potential at turgor loss; leaf osmotic potential at full turgor ($\Psi\pi_{100}$), the solute concentration in
228 leaf cells at full hydration; and modulus of elasticity (ε), cell wall stiffness.
229 Leaf mass per area (LMA) and leaf area to sapwood area ratios (A_L:A_S) were measured
230 using the collected foliage from the branch samples. Total one-sided leaf area (A_L) was
231 quantified with a LI-3100C area meter (Li-Cor Biosciences) and ImageJ (Schneider et al. 2012).
232 Leaves were then dried in a 60°C oven and dry weights recorded using a mass balance. LMA
233 was calculated by dividing dry weight by A_L. A_L:A_S was calculated by dividing A_L by the
234 sapwood diameter at the basal end of the branch segment.
235 One increment core was collected at breast height from focal trees. Cores were mounted
236 and sanded with progressively finer sandpaper until ring-width boundaries were visible under a
237 microscope. Cross dating was verified at the $P < 0.01$ significance level and using a 50-year
238 window which overlapped by 25 years in the program COFECHA (Holmes 1983). The "dplR"

(version 1.7.2) R package was used to convert raw ring widths to basal area increment (BAI) (Bunn 2008) which were used to build chronologies (Table S5, Fig. S1).

Common garden

Growth (height and stem diameter) was measured at the beginning and end of the 2020 growing season, and every 3 weeks during the 2021 growing season. Relative growth rate in height (RGR_{height}) and diameter (RGR_{dia}) was determined for the full irrigation period prior to the drought treatment using equation 2:

$$RGR = [\frac{\ln(S_2) - \ln(S_1)}{(t_2 - t_1)}] \quad (2)$$

where S_2 and S_1 are the size (height or diameter) of the propagule taken at two time points, t_2 and t_1.

Leaf water potential and midday stomatal conductance were measured once a week during the 2021 drought experiment. A subset of plants was randomly selected to ensure there was representation from all clones/populations and that plants were not completely defoliated. Leaf water potential was measured during predawn (03:30 - 05:30) and midday (13:00 - 15:00). One fully developed leaf per plant was placed in a plastic bag prior to stem removal and then immediately measured with a pressure chamber (PMS Instruments). Stomatal conductance to water vapor (g_s) was measured on one fully developed intact leaf per plant during midday (full sun, 13:00 – 15:00) using a porometer (SC1 Leaf Porometer, Meter).

Gas exchange measurements were made at the end of the experiment to construct photosynthetic CO_2-response (A-C_i) curves for determination of maximum rate of carboxylation (V_{cmax}) using a portable open gas exchange system with a 6 cm^2 aperture and a red-blue light source (Li-6800, Li-Cor Biosciences). Environmental conditions in the Li-6800 were as follows: leaf temperature at 25°C, photosynthetic photon flux density at 2000 μmol m^{-2} s^{-1}, relative humidity at 50%, and ambient CO_2 concentration at 400 p.p.m. CO_2 concentration was initially set to ambient, then was gradually decreased stepwise to 50 p.p.m., brought back to ambient, then gradually increased stepwise until the curve reached a point where further increases in photosynthesis (A) appeared to be negligible. At each step, stabilized readings of A, stomatal conductance (g_s), and internal concentration of CO_2 (C_i) were recorded. The "plantecophys" (version 1.4.6) R package was used to fit A-C_i curves and determine V_{cmax} (Duursma 2015). We

corrected temperature for each curve to match the recorded leaf temperatures of the Li-6800 and used the default method for curve fitting.

Measurements of chlorophyll fluorescence taken at the end of the experiment were used to determine T_{50}, the temperature that causes 50% damage to photosystem II (PSII) (Krause et al. 2010). One to two leaves were collected from six plants per population per treatment at predawn to ensure foliage was dark acclimated. Three 2.54 cm^2 leaf discs from each sample were placed in plastic bags and immersed for 15 minutes in preheated water baths set to various temperatures (25-61 °C in 4 °C increments). Different sets of discs were exposed to each temperature and then stored in the dark on moist filter paper along with untreated leaf discs which served as controls. Maximum quantum yield (F_v/F_m), which is a reliable measure of PSII function (Genty et al. 1989), was measured at room temperature with a fluorometer (FluorPen FP 100, Photon Systems Instruments, Czech Republic) 24 hours after temperature exposure. T_{50} was estimated by modelling the relationship between F_v/F_m and temperature using logistic nonlinear least squares models and the 'nls' function in the "stats" R package (Feeley et al. 2020).

All other measurements (LMA, A_L:A_S, PV parameters, $K_{s\text{-}nat}$, $K_{s\text{-}max}$, PLC, P_{50}) were determined at the end of the experiment on a subset of plants using the methods described above.

Statistics

To test for differences among the natural populations, linear mixed effects models were constructed to relate absolute measurement values to the fixed effect of population and the random effects of tree and/or or tree nested in clone as shown in equation 3:.

$$y_{ij} = \beta_0 + \beta_1 X_{ij} + u_i + v_j + \varepsilon_{ij} \quad (3)$$

where y is indexed by *i* for tree and by *j* for clone, X indicates the effect of population, *u* and *v* represent the random intercepts for tree and clone respectively, and ε represents random error.

Given potential large differences in micro- and macro-site factors, and the use of different tree genotypes in each population, significant trait differences among natural populations do not necessarily indicate genotype (G) or environment (E) effects. Data from the common garden was used to specifically investigate the effects of G, E, and GxE interactions on trait expression. Within the common garden, linear mixed effects models were constructed to relate absolute measurement values to the fixed effects of population and treatment (drought, control), and the random effects of clone or bed as shown in equation 4:.

$$y_{ij} = \beta_0 + \beta_1 X_{1ij} + \beta_2 X_{2ij} + \beta_1 X_{1ij} \times \beta_2 X_{2ij} + u_i + w_j + \varepsilon_{ij} \quad (4)$$

where y is indexed by *i* for clone and by *j* for bed, X_1 indicates the effect of population, X_2 indicates the effect of treatment, *u* and *w* represent the random intercepts for clone and bed respectively, and ε represents random error. Significant differences among populations within a treatment group indicate G effects, between treatment groups within a population indicate E effects, and models with a significant interaction term indicate GxE effects.

Model assumptions of normality were checked with diagnostic plots of residuals. For the cases when model assumptions were violated, a square-root (field $K_{s\text{-}spin}$), or log transformation was performed (garden A_L:A_S). Extreme outliers (e.g., flagged data of poor quality or incorrectly entered) were determined using the Cook's Distance method and removed from the field LMA and A_L:A_S datasets, and the garden LMA, P_{50}, and Ψ_{TLP} datasets, when necessary. The effects of population and/or treatment and/or their interaction were then determined with Likelihood Ratio Tests (LRT) by comparing the full model to reduced models (Table S6). When population and/or treatment proved to be significant, pairwise comparisons were made to test whether measurement values differed significantly among populations in the field datasets, and among populations within treatment or among treatments within populations in the garden datasets.

For the common garden, a phenotypic plasticity index was determined for growth and drought resistance traits (RGR_{height}, RGR_{dia}, LMA, A_L:A_S, Ψ_{TLP}, P_{50}, K_{max}, V_{cmax}, T_{50}) in each population (Valladares et al. 2000). The index was calculated as the difference between the minimum and maximum mean trait values within population across the two treatment groups divided by the maximum mean trait value as shown in equation 5:

$$\text{Plasticity index} = \frac{(\text{max} - \text{min})}{\text{max}} \quad (5)$$

An overall mean phenotypic plasticity index for each population was also calculated by averaging the individual trait phenotypic plasticity indexes. These indexes range from 0 (no plasticity) to 1 (maximum plasticity). The use of this plasticity index assumes trait data are normally distributed (Valladares et al. 2006) which we confirmed as described above.

To determine if there were growth-stress tolerance trade-offs, linear regressions were first used to test for significant relationships between growth (BAI in the field, and RGR_{dia} and RGR_{height} in the garden) and drought vulnerability (PLC or $K_{s\text{-}spin}$ in the field, and PLC, predawn water potential, or P_{50} in the garden). Tree age did not significantly affect BAI (Fig. S2). Linear regressions were then used to test for significant relationships between drought resistance traits

(field: LMA, A_L:A_S, Ψ_{TLP}, K_{nat}, K_{max}, $K_{s\text{-}spin}$, PLC; garden: LMA, A_L:A_S, Ψ_{TLP}, P_{50}, T_{50}, V_{cmax}, K_{nat}, K_{max}, PLC) and growth. To determine if mortality in natural populations was mediated by drought resistance traits, linear regression was used to test for significant relationships between traits (listed above) and 2021 % canopy dieback. Coefficients of determination (R^2) and p-values were determined through linear regressions.

Analyses were conducted in R version 4.1.2 (R Core Team 2021). The "lme4" (version 1.1.28), "lmerTest" (version 3.1.3), and "emmeans" (version 1.7.2) packages were used to construct and analyze mixed effects models (Bates et al. 2019; Kuznetsova et al. 2014; Lenth et al. 2018). Significance of fixed effects were determined with LRTs using "lmerTest" and the Satterthwaite approximation method. Pairwise comparisons were determined using "emmeans" and the Tukey method for p-value adjustments. The "car" package (version 3.0.12) was used to plot QQ normal lines with 95% confidence intervals for assumption validation (Fox et al. 2016). Significance levels of $\boldsymbol{\alpha} < 0.05$ and $\boldsymbol{\alpha} = 0.05$ - 0.1 were considered statistically significant and marginally significant, respectively.

Results

Natural populations

The five natural populations for this study spanned a macro-climate gradient that ranged hotter/drier in southern latitudes to cooler/wetter in northern latitudes (Fig. 1a, Table S1). Populations that were more geographically isolated (i.e., Dixie) were also more genetically distinct (Fig. 1b).

There were significant intraspecific differences in trait measurements. Population had a strong effect on LMA ($\boldsymbol{\chi}^2$=230.95, p<0.0001), A_L:A_S ($\boldsymbol{\chi}^2$=50.378, p<0.0001), $K_{s\text{-}spin}$ ($\boldsymbol{\chi}^2$=38.404, p<0.0001), and PLC ($\boldsymbol{\chi}^2$=30.724, p<0.0001). Aspen from Dixie and San Juan, the two hotter/drier populations, generally had significantly lower LMA (Fig. 2a), higher A_L:A_S (Fig. 2b), and lower hydraulic conductivity after receiving the cavitation-inducing pressure of -2.5 MPa ($K_{s\text{-}spin}$, Fig. 2c) than their cooler/wetter counterparts. PLC was highest in Dixie and San Juan aspen (Fig. 2f) which suggests heightened drought stress during summer 2020 despite lower maximum hydraulic conductivity (Fig. 2e). There was no population-level variation in Ψ_{TLP} ($\boldsymbol{\chi}^2$=2.4352, p=0.6563, Fig. 2d). Ψ_{TLP} was measured during 2021 which, despite being a

generally hot and dry year, had erratic rainfalls that likely disrupted drought signals that would result in differences in Ψ_{TLP} at the time of measurement.

Common garden

Summer 2021 had higher than average rainfall, which resulted in two sporadic recovery events and a mild-to-moderate drought treatment. Yet predawn (χ^2=95.223, p<0.001) and midday (χ^2=50.589, p<0.001) xylem pressures (Fig. S3a), midday stomatal conductance (χ^2=76.041, p<0.001, Fig. S3b), and soil moisture levels (χ^2=146.19, p<0.001, Fig. S3c) were significantly lower in drought treatment propagules indicating these plants did experience heightened drought stress compared to control plants.

In general, there were little to no treatment and population-level differences in traits which indicated limited G, E, or GxE effects. We only observed significant treatment (E) in Ψ_{TLP} and weak GxE differences in T_{50} (Fig. 3). The drought treatment had a significant E effect on Ψ_{TLP} for all propagules (χ^2=17.959, p=0.003), whereby Ψ_{TLP} was less negative in plants under drought regardless of their population of origin (Fig. 3e). Among the Dixie propagules, T_{50} was reduced in plants under drought (p=0.0152, Fig. 3f) suggesting a GxE effect. Although the T_{50} linear mixed effects model did not have significant G,E,or GxE terms (Table S6), we thought these results deserved further investigation given the sharp decline in T_{50} in propagules subjected to the drought. Pairwise comparisons confirmed T_{50} in the Dixie propagules was statistically significant between the treatments and therefore possibly the result of a GxE effect.

Plasticity index values for drought resistance traits were generally low, ranging from 0.05 (LMA) to 0.45 (RGR_{height}) across all populations (Fig. S4). Propagules from the hotter/drier populations (Dixie and San Juan) varied widely in plasticity. Dixie propagules consistently exhibited the lowest plasticity indexes across all traits while San Juan propagules had some of the highest plasticity indexes in hydraulic conductance and growth (Fig. S4). The overall mean plasticity index across all traits did not vary strongly with population and was also generally low (Fig. 4). Dixie propagules did have a significantly lower mean plasticity index (p=0.045) compared to San Juan propagules despite both groups originating from similar hot/dry climates (Fig. 4).

Trait-mediated trade-offs

In the common garden, we found no evidence of a growth-stress tolerance trade-off between propagules with more growth (higher RGR_{height} and RGR_{dia}) under full irrigation prior to the drought treatment compared to xylem vulnerability (less negative P_{50}) during the drought treatment (Fig. 5). There were also no trade-offs between growth and the other metrics of xylem vulnerability we tested (PLC and predawn water potential during drought). Among the natural populations, we also did not find strong evidence of a growth-stress tolerance trade-off where trees with higher growth (BAI) during a timeframe with more rainfall (1980 -1999) had more vulnerable xylem during 2020 (i.e., higher PLC or $K_{s\text{-}spin}$). Yet this trade-off did occur in trees from Uncompaghre and White River, which exhibited a significant (R^2=0.24, p=0.012) and marginally significant (R^2=0.17, p=0.054) positive linear relationship between BAI and PLC, respectively (Fig. 6). These same trees did not experience increased mortality (i.e., canopy dieback scored in 2021) following the 2020 drought (Fig. S5, R^2=0.13, p=0.548).

In the common garden, trait data were pooled across treatments for trait-trait correlations due to the lack of observed significant trait differences between the control and drought treatments. We did observe some significant linear relationships that indicate possible physiological trade-offs among the propagules tested here (see Fig. S6 for all trait-trait comparisons made). There appeared to be safety-efficiency trade-off as propagules with more efficient xylem (higher $K_{s\text{-}nat}$ and $K_{s\text{-}max}$) were more vulnerable to drought (less negative P_{50}). This evidence is provided by statistically significant linear relationships between both P_{50} and $K_{s\text{-}nat}$ (R^2=0.19, p<0.001, Fig. 7a) and P_{50} and $K_{s\text{-}max}$ (R^2=0.22, p<0.001, Fig. 7b). In addition, the linear relationship between P_{50} and T_{50} was statistically significant (R^2=0.12, p<0.001, Fig. 7c) indicating that propagules with more resistant xylem (more negative P_{50}) had improved heat tolerance (higher T_{50} temperatures).

Among the natural populations, there were significant linear relationships between three traits and percent canopy dieback in 2021 (see Fig. S7 for all trait-trait comparisons made). $K_{s\text{-}nat}$ (R^2=0.17, p=0.029, Fig. 7d), $K_{s\text{-}max}$ (R^2=0.21, p=0.014, Fig. 7e), and LMA (R^2=0.18, p=0.022, Fig. 7f) all exhibited statistically significant linear relationships with canopy dieback. These results suggest that trees with thinner, wider leaves (lower LMA) that were less hydraulically efficient (lower Ks-nat and $K_{s\text{-}max}$) during the severe 2020 drought experienced increased mortality the following growing season.

Discussion

Overall, we found large intraspecific drought resistance trait variation among the natural populations, limited evidence for G and E effects in the garden, generally low plasticity yet evidence for safety-efficiency trade-offs in the garden, and relatively few trait-mediated growth-drought tolerance trade-offs in both the natural populations and garden. Taken together, our results highlight an unexpected decoupling of physiological traits from demographic performance (i.e., growth and mortality). Specifically, we discovered that traits measured in mature aspen trees from hotter/drier populations (Dixie and San Juan) were not indicative of these populations having more drought tolerance than their cooler/wetter counterparts. In addition, mature trees and propagules that grew more during wetter time periods generally did not exhibit increased vulnerability to drought, possibly suggesting little growth-stress tolerance trade-offs. Among the natural populations, only leaf mass per area (LMA) and hydraulic conductivity seemed to be important traits in mediating mortality following drought. These results underscore the persistent challenges of using saplings to infer mature tree response, connecting physiological traits to demographic responses (Greenwood et al. 2017, Laughlin et al. 2020) and the temporal disconnect between the onset of drought and mortality (Trugman et al. 2018).

Natural populations

Despite evidence of genotypic differentiation, the intraspecific variation seen here in drought resistance functional traits was often counterintuitive to hypotheses regarding local adaptation. If local adaptation was present, hotter/drier populations would have stronger drought resistance traits to allow these trees to deal with the water stress limitations inherent at those sites. Instead, we found that trees from these populations had thinner leaves, more leaf area, and xylem that was more vulnerable to drought, although this study did not account for belowground processes such as rooting depth or groundwater subsidies (Love et al. 2019) that may mediate drought resistance traits. Previous work has shown similar counterintuitive results, as aspen growing in hotter/drier environments were found to have more leaf area during a drought that correlated with increased canopy dieback (Kerr et al. 2022) and triploids have been shown to have higher growth and more risky hydraulic behavior that may increase risk of drought-induced mortality (DeRose et al. 2014, Greer et al. 2017, Blonder et al. 2022). In this present study, the

production of more leaf area and thinner, wider leaves was likely mal-adaptive and may have been due to a "structural overshoot" (Jump et al. 2017) where increased aboveground growth becomes temporally mismatched with water availability. Overproduction of low LMA foliage may have been due to climatic conditions during vegetative bud set the previous growing season or advanced phenology due to warmer spring temperatures in 2020 (Gordo and Sanz 2010). Alternatively, poor drought resistance may be adaptive in this species if there is more rapid regrowth post-drought (DeRose et al. 2014), yet long term trends in aspen demography suggest a net loss of aspen regrowth and basal area in recent decades (Refsland and Cushman 2020).

The Dixie and San Juan populations reside in the northern transition zone of the North American Monsoon (NAM) precipitation pattern, and disruption to the NAM due to climate change may be driving more variable climatic signals that influence leaf production (Pascale et al. 2017). However, sapwood growth was not complete at the time of measurement which would alter several traits (e.g., A_L:A_S, $K_{s\text{-}max}$, K_{spin}) and emphasizes the importance of intra-annual variability for complete understanding of *in-situ* drought resistance. Furthermore, traits reported here are namely branch-level measurements that may not be reflective of whole-plant drought response, and future work could focus on the intra-individual trait variation and coordination of traits at the whole-plant level to assess a species' ability to cope with future drought stress (Herrera 2017, McCulloh et al. 2019, Cardoso et al. 2020, Johnson et al. 2021).

Common garden

Achieving our target predawn leaf water potential target of -1 MPa for propagules in drought beds was difficult as propagules did not become water stressed as quickly as we anticipated, and unprecedented rain events disrupted drought signals. Thus, while the drought treatment was statistically significant with respect to leaf water potential, plant midday stomatal conductance, and soil water (Fig. S3), results from the common garden are likely reflective of responses to mild-to-moderate drought stress and not severe drought conditions.

Plasticity index values were generally small (i.e., low plasticity) for the growth and traits we measured, especially for propagules from hottest/driest population, which may indicate aspen from this population are unable to adjust to more extreme drought conditions (Valladares et al. 2007). These results contrast studies that have shown high phenotypic plasticity in aspen growth and functional traits (St. Clair *et al.*, 2010; Cope *et al.*, 2020; Fedorkov *et al.*, 2021, but see

485 Kanaga *et al.*, 2008 for evidence of stronger genetic control), which may be explained by a
486 difference in traits studies or that Colorado and Utah have overall dry climates that may pose
487 strong selective filters that minimize plastic potential. This study only determined plasticity
488 across two contrasting environments, and future work could include a larger number of diverse
489 environments to obtain a more complete understanding of plasticity. Results from the linear
490 mixed effects models suggest that neither genotype (G), environment (E), or their interaction
491 (GxE) were strongly influential on traits as we generally observed no differences among the
492 populations (G effects) or across the treatments (E effects). Stronger G, E, and GxE effects may
493 have been elicited under a stronger drought treatment. Despite the mild-to-moderate drought,
494 Ψ_{TLP} (leaf water potential at turgor loss) in all populations was affected by the treatment (E
495 effect) and T_{50} (temperature that caused a 50% reduction in photosystem II function) in the Dixie
496 population was affected by a GxE interaction.
497 The occurrence of less negative Ψ_{TLP} in plants under drought was unexpected as species
498 typically exhibit more negative Ψ_{TLP} in response to drought making it a strong indicator of
499 ecological drought tolerance (Bartlett et al. 2012). These results may be explained by differences
500 in biomass allocation whereby propagules in the drought treatment had possibly longer root
501 systems that were able to access deeper water sources to maintain leaf turgor under drought
502 stress (Fig. S8). Midday stomatal conductance was significantly depressed in drought treatment
503 propagules, and these propagules may have had some depletion of nonstructural carbohydrates
504 (NSCs) that reduced the concentration of soluble sugars required for osmoregulation (Woodruff
505 and Meinzer 2011, Sevanto et al. 2014). Osmotic potential at full turgor showed a strong linear
506 relationship with Ψ_{TLP}, which indicates osmotic adjustment was a primary mechanism driving
507 Ψ_{TLP} in these propagules (Fig. S9). Measuring NSCs may have provided a better understanding
508 of the carbon dynamics at play, although the presence of NSCs may not necessarily mean they
509 are osmotically active and available for osmotic adjustment (Morgan 1984). These results may
510 also be reflective of ontogeny, whereby young trees may prioritize growth or other aspects of
511 fitness over drought resistance compared to mature trees.
512 Dixie propagules in the control group had the highest, albeit not significantly, T_{50} values.
513 The Dixie NF represented the driest/hottest population among our climate gradient which could
514 indicate the differences in thermal tolerance observed here are due to genotype effects and
515 perhaps a mechanism of local adaption to hot conditions. Other studies have found heat tolerance

to be more phenotypically plastic and representative of responses to the growing environment (Marias et al. 2017, Feeley et al. 2020). We observed a strong shift in T_{50} between Dixie propagules in the control and drought treatments, suggesting this trait was also highly plastic or subject to GxE interactions within this population. There may also have been micro-climate differences among the garden beds or biophysical differences in leaf structure that resulted in the control treatment Dixie propagules experiencing possibly more extreme leaf temperatures and increased heat tolerance (Perez and Feeley 2020). The large reduction in T_{50} in Dixie propagules under the drought treatment may be explained by the accompanied reduction in available water. Water transport through xylem and high stomatal conductance are likely important heat transfer mechanisms that cool plants to prevent lethal temperatures from occurring (Kolb and Robberecht 1996).

Trade-offs

Despite expectations from classic ecological theory, we did not find evidence of a growth-stress tolerance trade-off in the common garden nor most of the natural populations. In the garden, propagules that grew more under wet conditions prior to the drought treatment did not have xylem that was more vulnerable to drought, which may have been due to the mildness of the drought treatment. In the natural populations, a general lack of growth-stress tolerance trade-offs may have been due to the relatively smaller geographic scale of this work as these types of trade-offs tend to be observed at larger geographic scales (e.g., across entire species distributions, Anderegg and HilleRisLambers 2019) or due to belowground processes like rooting depth and groundwater subsidies (Love et al. 2019). Alternatively, despite sampling only mature aspen trees, there may have been variation in stand development we did not account for in our analyses that possibly confounded signals of lifetime growth strategies (DeRose et al. 2014). There was a significant trade-off in the Uncompaghre NF where aspen with more growth during the wetter years of 1980-1999 had xylem that was more vulnerable to the 2020 drought. However, these trees did not exhibit elevated levels of canopy dieback following the drought. This could be because aspen mortality can lag drought up to 5 years (Trugman et al. 2018) or that we collected tree rings that had survived to the present, biasing against trees that had been susceptible to previous drought-induced mortality events. These results could also be indicative of the trade-off not being strong enough to result in long-lasting changes in xylem vulnerability

or that climate change in the region, which is largely manifested as more extreme arid conditions, may overwhelm any trade-offs that affect drought resistance (Choat et al. 2012). Indeed, mortality in 2021 was strongly linked to growth that occurred during the most recent severe drought (2018) as canopy dieback was highest in the driest population despite trees in the Dixie NF also having the lowest growth in 2018 (Fig S5b).

We did find evidence of several trait relationships in both the common garden and natural populations that could influence drought stress resistance and susceptibility to drought-induced mortality. In the common garden, we observed a significant linear relationship between T_{50} and P_{50} indicating propagules with higher heat tolerance had more embolism-resistant xylem. High temperatures regularly accompany periods of drought stress (Williams et al. 2013), and therefore heat tolerance may be an important trait to consider in future studies that evaluate trait variation and aspen drought response. We also observed a safety-efficiency trade-off whereby propagules with higher hydraulic conductivity had xylem that was more vulnerable to cavitation (less negative P_{50}). These propagules likely had xylem with larger diameters (and/or thinner cell walls and/or more pits) which allowed them to be more efficient in water transport but more vulnerable to drought stress (Tyree and Sperry 1989). Adult aspen trees in the natural populations did not exhibit the same safety-efficiency trade-off as trees with higher conductivity were less vulnerable to drought stress. Differing hydraulic strategies may occur at different life stages in this species which would have implications for scaling from branch-level estimates of hydraulic safety and efficiency to the whole-plant (Meinzer et al. 2010). In addition, hydraulic measurements utilized all growth rings in the branch samples, and safety-efficiency relationships may be different if only current-year or ring-specific conductance were assessed (Melcher et al. 2003). The lack of a safety-efficiency trade-off among the natural populations did not preclude trees from mortality as we still observed increased canopy dieback among aspen trees native to hotter/drier climates following the severe drought of 2020. Tree mortality can be due to a multitude of factors, including previous droughts and interactions with biotic agents. Aspen from the hotter/drier populations, regions that regularly experience severe droughts, may have been unable to regrow enough damaged water transport tissue and were therefore more susceptible to drought-induced mortality in 2020 (Trugman et al. 2018). Future work could focus on inclusion of belowground traits/processes and traits that may indirectly affect drought response (i.e., defense traits) to gain a more complete understanding of aspen drought response and mortality.

Conclusion

We found that despite high intraspecific variation in drought resistance among natural aspen populations, functional traits were unexpectedly decoupled from demographic rates of growth and drought stress tolerance in the field and in a common garden. These results enhance our understanding of aspen physiological response to drought stress, the possible influences of genotype (G), environment (E), and GxE on functional trait expression, and the limits of drought resistance traits in this species. This knowledge can improve our ability to predict the future of western US forests in a changing climate by incorporating intraspecific trait variation in ecosystem models (Anderegg 2015, Tai et al. 2017). Results can also be applied to potential propagation programs that utilize natural aspen populations for restoration and assisted migration efforts. This work also highlights the persistent challenge of connecting drought response physiological traits to demographic rates, a field of research that could also improve forest forecasting efforts.

Acknowledgments

The authors thank Jaycee Cappaert, Coleson Kastelic, Shelby Jenkins, Nicole Zenes, Martin Venturas, April Radford, and Annapurna Post-Leon for their assistance with field and laboratory work. K.L.K. acknowledges support from the University of Utah Global Change and Sustainability Center, and the University of Utah Rio Mesa Center. W.R.L.A. acknowledges funding from the David and Lucille Packard Foundation, NSF Grants 1714972, 1802880, 2003017, and 2044937, and the USDA National Institute of Food and Agriculture, Agricultural and Food Research Initiative Competitive Programme, Ecosystem Services and Agro-ecosystem Management, Grant no. 2018-67019-27850.

Conflict of Interest

The authors do not declare any conflicts of interest.

Authors' Contributions

The experiment was designed by all authors. Data collection and analyses were carried out by KLK and JCF, while data interpretation was carried out by all authors. KLK led the writing of the manuscript, and all authors contributed to drafts and gave final approval for publication.

Data Availability Statement

Data will be deposited in the TRY and Dryad digital databases upon acceptance.

References

Adler, P.B., R. Salguero-Gómez, A. Compagnoni, J.S. Hsu, J. Ray-Mukherjee, C. Mbeau-Ache, and M. Franco. 2014. Functional traits explain variation in plant lifehistory strategies. Proceedings of the National Academy of Sciences of the United States of America **111**: 740–745.

Aitken, S.N., S. Yeaman, J.A. Holliday, T. Wang, and S. Curtis-McLane. 2008. Adaptation, migration or extirpation: climate change outcomes for tree populations. Evolutionary Applications **1**: 95–111.

Alder, N. N., W. T. Pockman, J. S. Sperry, and S. Nuismer. 1997. Use of centrifugal force in the study of xylem cavitation. Journal of Experimental Botany **48**: 665–674.

Allen, C. D., D. D. Breshears, and N. G. McDowell. 2015. On underestimation of global vulnerability to tree mortality and forest die-off from hotter drought in the Anthropocene. Ecosphere **6**: 1–55.

Amici, A. A., N. M. Nadkarni, E. DiBlasi, and J. Seger. 2019. Constrasting effects of host tree isolation on population connectedness in two tropical epiphytic bromeliads. American Journal of Botany **106**: 1602-1611.

Anderegg, L. D. L., W. R. L. Anderegg, J. Abatzoglou, A. M. Hausladen, and J. A. Berry. 2013. Drought characteristics' role in widespread aspen forest mortality across Colorado, USA. Global Change Biology **19**: 1526–1537.

Anderegg, W. R. L. 2015. Spatial and temporal variation in plant hydraulic traits and their relevance for climate change impacts on vegetation. New Phytologist 205:1008-1014.

Anderegg, L. D. L., and J. HilleRisLambers. 2019. Local range boundaries vs. large-scale trade-offs: climatic and competitive constraints on tree growth. Ecology Letters.

Anderegg, W. R. L., J. A. Berry, D. D. Smith, J. S. Sperry, L. D. L. Anderegg, and C. B. Field. 2012. The roles of hydraulic and carbon stress in a widespread climate-induced forest die-off. Proceedings of the National Academy of Sciences 109:233–237.

Bartlett, M. K., C. Scoffoni, and L. Sack. 2012. The determinants of leaf turgor loss point and prediction of drought tolerance of species and biomes: a global meta-analysis. Ecology Letters 15:393–405.

Bartlett, M. K., Y. Zhang, N. Kreidler, S. Sun, R. Ardy, K. Cao, and L. Sack. 2014. Global analysis of plasticity in turgor loss point, a key drought tolerance trait. Ecology Letters 17:1580–1590.

Bates, D., M. Maechler, B. Bolker, S. Walker, R. H. B. Christensen, H. Singmann, B. Dai, F. Scheipl, G. Grothendieck, … , J. Fox. 2019. Package 'lme4': Linear Mixed-Effects Models using "Eigen" and S4. CRAN Repository:1–123.

Blackman, C. J., M. J. Aspinwall, D. T. Tissue, and P. D. Rymer. 2017. Genetic adaptation and phenotypic plasticity contribute to greater leaf hydraulic tolerance in response to drought in warmer climates. Tree Physiology 37:583–592.

Bradshaw, A. D. 1965. Evolutionary Significance of Phenotypic Plasticty in Plants. Advances in Genetics 13:115–155.

Blonder B., P. G. Brodrick, J. A. Walton, K. D. Chadwick, I. K. Breckheimer, S. Marchetti, C. A. Ray, K. E. Mock. 2022. Remote sensing of cytotype and its consequences for canopy damage in quaking aspen. Global Change Biology 28:2491-2504.

Bunn, A. G. 2008. A dendrochronology program library in R (dplR). Dendrochronologia 26:115–124.

Cardoso A. A., T. A. Batz, S. A. M. McAdam. 2020. Xylem embolism resistance determines leaf mortality during drought in *Persea americana*. Plant Physiology 182:547-554.

Choat, B., S. Jansen, T. J. Brodribb, H. Cochard, S. Delzon, R. Bhaskar, S. J. Bucci, T. S. Feild, S. M. Gleason, … , A. E. Zanne. 2012. Global convergence in the vulnerability of forests to drought. Nature 491:752–755.

Clark, L. V., and M. Jasieniuk. 2011. Polysat: an R package for polyploid microsatellite analysis. Molecular Ecology Resources 11:562-566.

Cope, O. L., R. L. Lindroth, A. Helm, K. Keefover-Ring, and E. L. Kruger. 2020. "Trait plasticity and tradeoffs shape intraspecific variation in competitive response in a foundation tree species." New Phytologist.

Dai, A. 2013. Increasing drought under global warming in observations and models. Nature Climate Change 3:52–58.

DeRose R. J., K. E. Mock, J. N. Long. 2014. Cytotype differences in radial increment provide novel insight into aspen reproductive ecology and stand dynamics. Canadian Journal of Forest Research 45:1-8.

Duursma, R. A. 2015. Plantecophys - An R package for analysing and modelling leaf gas exchange data. PLoS ONE 10:1–13.

Duursma, R., and B. Choat. 2017. fitplc - an R package to fit hydraulic vulnerability curves. Journal of Plant Hydraulics 4:002.

Fedorkov, A., L.G. Stener, and P. Pulkkinen. 2021. Plasticity and stability of hybrid aspen clones in 14 field trials over Sweden, Finland and north-west Russia. Folia Forestalia Polonica 63:176–182.

Feeley, K., J. Martinez-Villa, T. Perez, A. Silva Duque, D. Triviño Gonzalez, and A. Duque. 2020. The Thermal Tolerances, Distributions, and Performances of Tropical Montane Tree Species. Frontiers in Forests and Global Change 3:1–11.

Fox, J., S. Weisberg, B. Price, D. Adler, D. Bates, G. Baud-bovy, B. Bolker, S. Ellison, D. Firth, … , R-Core. 2016. Package 'car': Companion to Applied Regression. CRAN Repository:1–147.

Franks, S. J., J. J. Weber, and S. N. Aitken. 2014. Evolutionary and plastic responses to climate change in terrestrial plant populations. Evolutionary Applications 7:123–139.

Genty, B., J.-M. Briantais, and N. R. Baker. 1989. The relationship between the quantum yield of photosynthetic electron transport and quenching of chlorophyll fluorescence. Biochimica et Biophysica Acta 990:87–92.

Gordo, O., and J. J. Sanz. 2010. Impact of climate change on plant phenology in Mediterranean ecosystems. Global Change Biology 16:1082–1106.

Greenwood S., P. Ruiz-Benito, J. Martinez-Vilalta, F. Lloret, T. Kitzberger, C. D. Allen, R.

Fensham, D. C. Laughlin, J. Kattge, … , A. S. Jump. 2017. Tree mortality across biomes in promoted by drought intensity, lower wood density and higher specific leaf area. Ecology Letters 20:539-553.

Greer B. T., C. Still, G. L. Cullinan, J. R. Brooks, F. C. Meinzer. 2017. Polyploidy influences plant-environment interactions in quaking aspen (*Populus tremuloides* Michx.). Tree Physiology 38:630-640.

Grime, J. P. 1977. Evidence for the Existence of Three Primary Strategies in Plants and Its Relevance to Ecological and Evolutionary Theory. The American Naturalist 111:1169–1194.

Herrera C. M. 2017. The ecology of subindividual variability in plants: patterns, processes, and prospects. Web Ecology 17:51-64.

Holmes, R. L. 1983. Program COFECHA user's manual. Laboratory of Tree-Ring Research, University of Arizona, Tucson, Arizona.

Jackson R. B., J. S. Sperry, T. E. Dawson. 2000. Root water uptake and transport: using physiological processes in global predictions. Trends in Plant Science 5:482-488.

Johnson K. M., C. Lucani, T. J. Brodribb. 2022. *In vivo* monitoring of drought-induced embolism in *Callitris rhomboidea* trees reveals wide variation in branchlet vulnerbility and high resistance to tissue death. New Phytologist. 233:207-218.

Jombart, T. 2008. Adegenet: A R package for the multivariate analysis of genetic markers. Bioinformatics 24:1403–1405.

Jump, A. S., and J. Peñuelas. 2005. Running to stand still: Adaptation and the response of plants to rapid climate change. Ecology Letters 8:1010–1020.

Jump, A. S., P. Ruiz-Benito, S. Greenwood, C. D. Allen, T. Kitzberger, R. Fensham, J. Martínez-Vilalta, and F. Lloret. 2017. Structural overshoot of tree growth with climate variability and the global spectrum of drought-induced forest dieback. Global Change Biology 23:3742–3757.

Kanaga, M. K., R. J. Ryel, K. E. Mock, and M. E. Pfrender. 2008. Quantitative-genetic variation in morphological and physiological traits within a quaking aspen (Populus tremuloides) population . Canadian Journal of Forest Research 38:1690–1694.

Kavanagh, K. L., B. J. Bond, S. N. Aitken, B. L. Gartner, and S. Knowe. 1999. Shoot and root vulnerability to xylem cavitation in four populations of Douglas-fir seedlings. Tree Physiology 19:31-37.

Kerr, K. L., F. C. Meinzer, K. A. Mcculloh, D. R. Woodruff, and D. E. Marias. 2015. Expression of functional traits during seedling establishment in two populations of Pinus ponderosa from contrasting climates. Tree Physiology 35:535–548.

Kerr, K. L., Anderegg, L. D. L., Zenes, N., and W. R. L. Anderegg. 2022. Quantifying within-species trait variation in space and time reveals limits to trait-mediated drought response. Functional Ecology 00:1-13.

Knight, C. A., and D. D. Ackerly. 2002. An ecological and evolutionary analysis of photosynthetic thermotolerance using the temperature-dependent increase in fluorescence. Oecologia 130:505-514.

Koide, R. T., R. H. Robichaux, S. R. Morse, and C. M. Smith. 1989. Plant water status, hydraulic resistance and capacitance. Pages 161–183 *in* P. R.W., E. J.R., M. H.A., and R. P.W., editors. Plant Physiological Ecology. Springer, Dordrecht.

Kolb, P. F., and R. Robberecht. 1996. High temperature and drought stress effects on survival of Pinus ponderosa seedlings. Tree Physiology 16:665–672.

Krause, G. H., K. Winter, B. Krause, P. Jahns, M. García, J. Aranda, and A. Virgo. 2010. High-temperature tolerance of a tropical tree, Ficus insipida: Methodological reassessment and climate change considerations. Functional Plant Biology 37:890–900.

Kuznetsova, A., P. B. Brockhoff, R. H. B. Christensen. 2017. lmerTest Package: Tests in Linear Mixed Effects Models. Journal of Statistical Software 82(13):1-26.

Lamy, J. B., S. Delzon, P. S. Bouche, R. Alia, G. G. Vendramin, H. Cochard, and C. Plomion. 2014. Limited genetic variability and phenotypic plasticity detected for cavitation resistance in a Mediterranean pine. New Phytologist 201:874–886.

Laughlin, D. C., J. R. Gremer, P. B. Adler, R. M. Mitchell, and M. M. Moore. 2020. The Net Effect of Functional Traits on Fitness. Trends in Ecology and Evolution 35(11):1037-1047.

Lenth, R. V. 2022. emmeans: Estimated Marginal Means, aka Least-Squares Means. R package version 1.7.5. https://CRAN.R-project.org/package=emmeans

López, R., U. López De Heredia, C. Collada, F. J. Cano, B. C. Emerson, H. Cochard, and L. Gil. 2013. Vulnerability to cavitation, hydraulic efficiency, growth and survival in an insular pine (Pinus canariensis). Annals of Botany 111:1167–1179.

Love, D. M., M. D. Venturas, J. S. Sperry, P. D. Brooks, J. L. Pettit, Y. Wang, W. R. L. Anderegg, X. Tai, and D. S. Mackay. 2019. Dependence of Aspen Stands on a Subsurface Water Subsidy: Implications for Climate Change Impacts. Water Resources Research 55:1833–1848.

Luna, T. 2003. Propagation protocol for aspen using root cuttings. NativePlants Fall:129–131.

Maherali, H., W. T. Pockman, and R. B. Jackson. 2004. Adaptive variation in the vulnerability of woody plants to zylem cavitation. Ecology 85:2184–2199.

Maherali, H., B. L. Williams, K. N. Paige, and E. H. Delucia. 2002. Hydraulic differentiation of Ponderosa pine populations along a climate gradient is not associated with ecotypic divergence. Functional Ecology 16:510–521.

Marias, D. E., F. C. Meinzer, D. R. Woodruff, and K. A. McCulloh. 2017. Thermotolerance and heat stress responses of Douglas-fir and ponderosa pine seedling populations from contrasting climates. Tree Physiology 37:301–315.

Martínez-Vilalta, J., H. Cochard, M. Mencuccini, F. Sterck, A. Herrero, J. F. J. Korhonen, P. Llorens, E. Nikinmaa, … , R. Zweifel. 2009. Hydraulic adjustment of Scots pine across Europe. New Phytologist 184:353–364.

McAvoy, D., M. Kuhns, and J. Black. 2012. Utah Forest Types: An Introduction to Utah Forests.

McCulloh K. A., J. C. Domec, D. M. Johnson, D. D. Smith, F. C. Meinzer. 2019. A dymanic yet vulnerable pipline: Integration and coordination of hydraulic traits across whole plants. Plant, Cell, and Environment 42:2789-2807.

Meinzer, F. C., K. A. McCulloh, B. Lachenbruch, D. R. Woodruff, D. M. Johnson. 2010. The blind men and the elephant: the impact of context and scale in evaluating conflicts between plant hydraulic safety and efficiency. Oecologia 164:287-296.

Melcher, P. J., M. A. Zwieniecki, N. M. Holbrook. 2003. Vulnerability of Xylem Vessels to Cavitation in Sugar Maple. Scaling from Individual Vessels to Whole Branches. Plant Physiology 131:1775-1780.

Mock, K. E., C. M. Callahan, M. N. Islam-Faridi, J. D. Shaw, H. S. Rai, S. C. Sanderson, C. A. Rowe, R. J. Ryel, … , P. G. Wolf. 2012. Widespread Triploidy in Western North American Aspen (Populus tremuloides). PLoS ONE 7:20–24.

Mock, K. E., C. A. Rowe, M. B. Hooten, J. Dewoody, and V. D. Hipkins. 2008. Clonal

dynamics in western North American aspen (Populus tremuloides). Molecular Ecology 17:4827–4844.

Morgan, J. M. 1984. Osmoregulation and Water Stress in Higher Plants. Annual Review of Plant Physiology 35:299–319.

Nicotra, A. B., O. K. Atkin, S. P. Bonser, A. M. Davidson, E. J. Finnegan, U. Mathesius, P. Poot, M. D. Purugganan, C. L. Richards, … , M. van Kleunen. 2010. Plant phenotypic plasticity in a changing climate. Trends in Plant Science 15:684–692.

Parker, W. C., and S. G. Pallardy. 1987. The influence of resaturation method and tissue type on pressure-volume analysis of Quercus alba L. seedlings. Journal of Experimental Botany 38:535–549.

Pascale, S., W. R. Boos, S. Bordoni, T. L. Delworth, S. B. Kapnick, H. Murakami, G. A. Vecchi, and W. Zhang. 2017. Weakening of the North American monsoon with global warming. Nature Climate Change 7:806–812.

Perez, T. M., and K. J. Feeley. 2020. Photosynthetic heat tolerances and extreme leaf temperatures. Functional Ecology 34:2236–2245.

Pritzkow, C., V. Williamson, C. Szota, R. Trouvé, and S. K. Arndt. 2020. Phenotypic plasticity and genetic adaptation of functional traits influences intra-specific variation in hydraulic efficiency and safety. Tree Physiology 40:215–229.

R Core Team. 2021. R: A language and environment for statistical computing. R Foundation for Statistical Computing, Vienna, Austria.

Refsland T. K., J. H. Cushman. 2020. Continent-wide synthesis of the long-term population dynamics of quaking aspen in the face of accelrating human impacts. Oecologia 197:25-42.

Reich, P. B. 2014. The world-wide "fast-slow" plant economics spectrum: A traits manifesto. Journal of Ecology 102:275–301.

Schneider, C. A., W. S. Rasband, and K. W. Eliceiri. 2012. NIH Image to ImageJ: 25 years of image analysis. Nature Methods 2012 9:7 9:671–675.

Sevanto, S., N. G. Mcdowell, L. T. Dickman, R. Pangle, and W. T. Pockman. 2014. How do trees die? A test of the hydraulic failure and carbon starvation hypotheses. Plant, Cell and Environment 37:153–161.

Sperry, J. S., M. D. Venturas, H. N. Todd, A. T. Trugman, W. R. L. Anderegg, Y. Wang, and X. Tai. 2019. The impact of rising CO2 and acclimation on the response of US forests to global warming. Proceedings of the National Academy of Sciences of the United States of America 116:25734–25744.

Sperry, J. S. K. L. Nichols, J. E. M. Sullivan, S. E. Eastlack. 1994. Xylem Embolism in Ring-Porous, Diffuse-Porous, and Coniferous Trees of Northern Utah and Interior Alaska. Ecology 75:1736-1752.

Sperry, J. S., J. R. Donnelly, and M. T. Tyree. 1988. A method for measuring hydraulic conductivity and embolism in xylem. Plant, Cell and Environment 11:35-40.

St. Clair, S. B., K. E. Mock, E. M. Lamalfa, R. B. Campbell, and R. J. Ryel. 2010. Genetic Contributions to Phenotypic Variation in Physiology, Growth, and Vigor of Western Aspen (Populus tremuloides) Clones. Forest Science 56.

Tai, X., D. S. Mackay, W. R. L. Anderegg, J. S. Sperry, P. D. Brooks. 2017. Plant hydraulics improves and topography mediates prediction of aspen mortality in southwestern USA. New Phytologist 213:113-127.

Thioulouse, J., and S. Dray. 2007. Interactive multivariate data analysis in R with the ade4 and ade4TkGUI packages. Journal of Statistical Software 22:1–14.

Trugman, A. T., L. D. L. Anderegg, W. R. L. Anderegg, A. J. Das, and N. L. Stephenson. 2021. Why is Tree Drought Mortality so Hard to Predict? Trends in Ecology and Evolution 36:520–532.

Trugman, A. T., M. Detto, M. K. Bartlett, D. Medvigy, W. R. L. Anderegg, C. Schwalm, B. Schaffer, and S. W. Pacala. 2018. Tree carbon allocation explains forest drought-kill and recovery patterns. Ecology Letters 21:1552–1560.

Tyree, M. T., and J. S. Sperry. 1989. Vulnerability of Xylem to Cavitation and Embolism. Annual Review of Plant Physiology and Plant Molecular Biology 40:19–38.

Valladares, F., E. Gianoli, and J. M. Gómez. 2007. Ecological limits to plant phenotypic plasticity. New Phytologist 176:749–763.

Valladares, F., D. Sanchez-Gomez, M. A. Zavala. 2006. Quantitative estimation of phenotypic plasticity: bridging the gap between the evolutionary concept and its ecological applications. Journal of Ecology 94:1103-1116.

Valladares, F., S. J. Wright, E. Lasso, K. Kitajima, and R. W. Pearcy. 2000. Plastic phenotypic response to light of 16 congeneric shrubs from a panamanian rainforest. Ecology 81:1925–1936.

Varone, L., M. Vitale, R. Catoni, and L. Gratani. 2016. Physiological differences of five Holm oak (Quercus ilex L.) ecotypes growing under common growth conditions were related to native local climate. Plant Species Biology 31:196–210.

Whitham, T. G., C. N. Slobodchikoff. 1981. Evolution by Individuals, Plant-Herbivore Interactions, and Mosaics of Genetic Variability: The Adaptive Significance of Somatic Mutations in Plants. Oecologia 49:287-292.

Williams, A. P., C. D. Allen, A. K. Macalady, D. Griffin, C. A. Woodhouse, D. M. Meko, T. W. Swetnam, S. A. Rauscher, R. Seager, … , N. G. Mcdowell. 2013. Temperature as a potent driver of regional forest drought stress and tree mortality. Nature Climate Change 3:292–297.

Williams, A. P., B. I. Cook, and J. E. Smerdon. 2022. Rapid intensification of the emerging southwestern North American megadrought in 2020–2021. Nature Climate Change 12:232–234.

Woodruff, D. R., and F. C. Meinzer. 2011. Water stress, shoot growth and storage of non-structural carbohydrates along a tree height gradient in a tall conifer. Plant, Cell and Environment 34:1920–1930.

Worrall, J. J., L. Egeland, T. Eager, R. A. Mask, E. W. Johnson, P. A. Kemp, and W. D. Shepperd. 2008. Rapid mortality of Populus tremuloides in southwestern Colorado, USA. Forest Ecology and Management 255:686–696.

Wright, I. J., P. B. Reich, M. Westoby, D. D. Ackerly, Z. Baruch, F. Bongers, J. Cavender-Bares, T. Chapin, J. H. C. Cornellssen, … , R. Villar. 2004. The worldwide leaf economics spectrum. Nature **428**: 821–827.

Figure Legends

Figure 1. Genetic variation between the aspen populations is associated with geographic distance. (**A**) Five natural populations of aspen were selected from National Forests (NF) in Utah and Colorado, USA: Dixie NF, San Juan NF, Uncompaghre NF, White River NF, and Uinta NF. (**B**) Principal Component Analysis showing variation in allele frequencies from 8 microsatellite

loci among clones within natural populations. Colors indicate population or geographic region of origin, and each point represents a genetically distinct clone (N=6 clones per population) and ellipses represent 95% confidence intervals.

Figure 2. Measurements taken during the severe drought of 2020 showed that aspen trees from the hotter/drier populations (Dixie and San Juan) had thinner leaves, more leaf area, and xylem that was more vulnerable to drought. Measurements include: leaf mass per area (**A**, LMA), the ratio of leaf area to sapwood area (**B**, A_L:A_S), hydraulic conductivity after a cavitation-inducing pressure of -2.5 MPa (**C**, $K_{s\text{-}spin}$), leaf water potential at turgor loss point (**D**, Ψ_{TLP}), maximum hydraulic conductivity (**E**, $K_{s\text{-}max}$), and percent loss of conductance (**F**, PLC). Boxplots (A-E) represent median values (center bar), interquartile ranges (IQR, box edges), values at most 1.5*IQR from box edge (error bars), and outlying points (circular points). Bars (F) represent mean PLC and error bars represent one standard error. Significant results have unique letters while nonsignificant results share the same letters. Statistical results have been omitted from E to aid in visual interpretation.

Figure 3. Measurements taken in the common garden at the end of the drought treatment showed low within-species and between-treatment differences. Leaf water potential at the turgor loss point (Ψ_{TLP}) was significant less negative in propagules that received the drought treatment, and the Dixie propagules had a significant reduction in temperature that caused 50% damage to photosystem II (T_{50}) under the drought treatment. Measurements include: leaf mass per area (**A**, LMA), the ratio of leaf area to sapwood area (**B**, A_L:A_S), maximum rate of carboxylation (**C**, V_{cmax}), pressure at which 50% loss of hydraulic conductivity occurs (**D**, P_{50}), Ψ_{TLP} (**E**), T_{50} (**F**), maximum hydraulic conductivity (**G**, $K_{s\text{-}max}$), and percent loss of conductance (**H**, PLC). Points represent mean values and error bars represent one standard error. The asterisks indicate statically significant differences where $p<0.05$. The black asterisk indicates a treatment-level significant result, and the yellow asterisk indicates a population-level significant result.

Figure 4. Mean plasticity indexes for each population across all the plasticity indexes for growth and drought resistance traits shown in Fig. S4. Bars represent mean plasticity index and error

907 bars represent one standard error. The asterisk indicates a significant difference between
908 propagules that originated from the Dixie and San Juan National Forests ($p < 0.05$).
909
910 **Figure 5**. Among the propagules that received a drought treatment in the common garden, there
911 was no significant trade-off between growth under wet conditions and survival under drought
912 conditions as indicated by the linear relationship between relative growth rate in height (**A**,
913 RGR_{height}) or diameter (**B**, RGR_{dia}) prior to the drought treatment and the pressure at which 50%
914 loss of hydraulic conductivity occurred (P_{50}) at the end of the drought treatment. Points represent
915 individual propagules that are colored according to the population (National Forest) of origin.
916 The black line represents a linear model regression fit (the coefficient of determination (R^2) and
917 p-value from the model are provided) and the grey shading represents a 95% confidence interval.
918
919 **Figure 6.** Among the natural populations, we observed growth-stress tolerance trade-offs in the
920 Uncompaghre (R^2=0.24, p=0.012) and White River (R^2=0.17, p=0.054) National Forests where
921 aspen with more growth (higher basal area increments, BAI) during wet periods (1980-1999) had
922 xylem that was more vulnerable to the 2020 severe drought (higher percent loss of conductance,
923 PLC). Points represent individual trees that are colored according to the population (National
924 Forest). The lines represent linear model regression fits (coefficients of determination (R^2), and
925 p-values models model are provided on each figure) which are also colored according to the
926 population. 95% confidence intervals have been omitted to aid in visual interpretation.
927
928 **Figure 7.** Trait-mediated trade-offs related to increased drought resistance occurred in both the
929 common garden and natural populations. In the common garden, propagules with less negative
930 pressures at which 50% loss of hydraulic conductivity occurred (P_{50}) had higher native (**A**, $K_{s\text{-}nat}$)
931 and maximum (**B**, $K_{s\text{-}max}$) hydraulic conductivity (i.e., more drought-vulnerable xylem).
932 Propagules with more negative P_{50} also tolerated higher temperatures before 50% damage to
933 photosystem II occurred (**C**, T_{50}). In the natural populations, aspen trees with lower native (**D**,
934 $K_{s\text{-}nat}$) and maximum (**E**, $K_{s\text{-}max}$) hydraulic conductivity, and lower leaf mass per area (**F**, LMA)
935 during the severe drought of 2020 experienced heightened canopy dieback (mortality) in 2021.
936 Points in A-C represent individual propagules, while points in D-F represent plot-level averages.
937 Black lines represent linear model regression fits (coefficients of determination (R^2), and p-

values models model are provided on each figure). Grey shading represents 95% confidence intervals. The seedling and tree icons indicate if the results occurred in the common garden or natural populations, respectively.

Table S1. Seasonal climate data for each population as estimated by TerraClimate.

Table S2. Microsatellite allele sizes and frequencies (Freq) for each locus observed in each population.

Table S3. F_{ST} values determined to estimate genetic variation among the 5 populations/national forests.

Table S4. Genotype table for mature aspen trees and garden propagules.

Table S5. Statistics for basal area increment (BAI) chronologies for each population/national forest.

Table S6. Analytical results for mixed-effects models.

Figure S1. Chronologies for each natural aspen population based on basal area increment (BAI) measurements.

Figure S2. Linear relationship between basal area increment (BAI) during the wetter years of 1980-1999 and tree age.

Figure S3. Measurements taken during the 2021 drought experiment in the common garden.

Figure S4. There were population-specific differences in trait plasticity index values although plasticity was typically low, especially among propagules that originated from the Dixie population.

Figure S5. Linear relationships between basal area increment BAI during the wetter years of 1980-1999 and canopy dieback in 2021 (**A**) and (BAI) during the severe drought year of 2018 and canopy dieback in 2021 (**B**).

Figure S6. Linear regressions for drought resistance traits measured at the end of the drought treatment compared with relative growth rate in height (RGR_{height}) prior to the drought treatment in the common garden.

Figure S7. Linear regressions for plot-level drought resistance traits compared with 2021 mortality (canopy dieback) among the natural populations.

Figure S8. At the end of the drought experiment, there was more aboveground growth in propagules within the control treatment compared to propagules within the drought treatment.

Figure S9. Linear relationships between end of drought treatment leaf water potential at the turgor loss point (Ψ_{TLP}) and leaf osmotic potential at full turgor (**A**, $\Psi\pi_{100}$), cell wall elasticity (**B**, ε), and apoplastic water fraction (**C**, AWF).

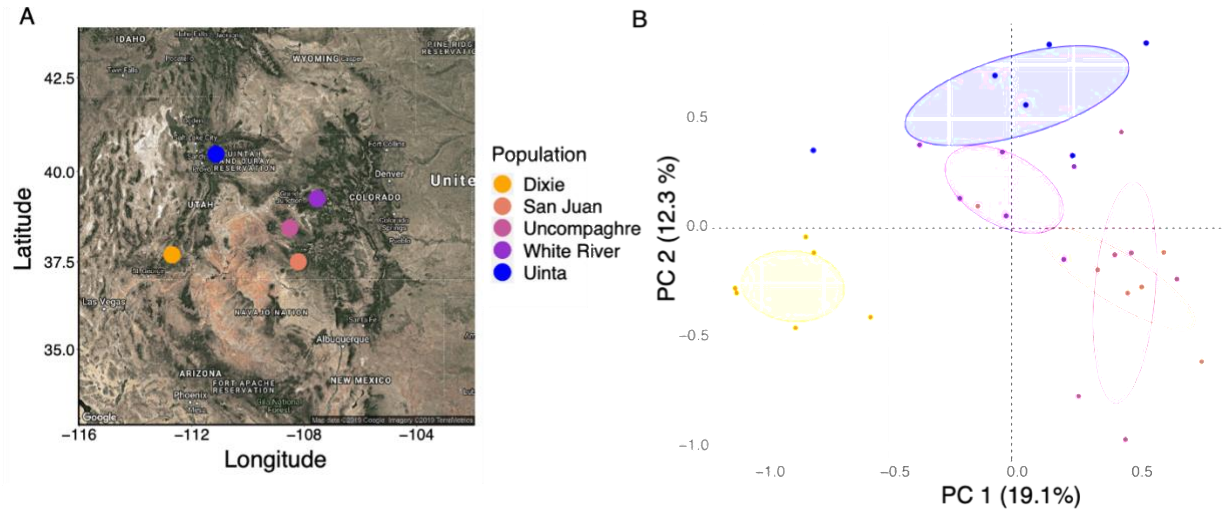

Figure 1. Genetic variation between the aspen populations seems to be driven by geographic distance. (**A**) Five natural populations of aspen were selected from National Forests (NF) in Utah and Colorado, USA: Dixie NF, San Juan NF, Uncompaghre NF, White River NF, and Uinta NF. (**B**) The two major axes of the principal components analysis indicate allele variation seems linked to geographic variation. Colored points indicate the geographic location of populations, and each point represents a genetically distinct clone (N=6 clones per population) and ellipses represent 95% confidence intervals.

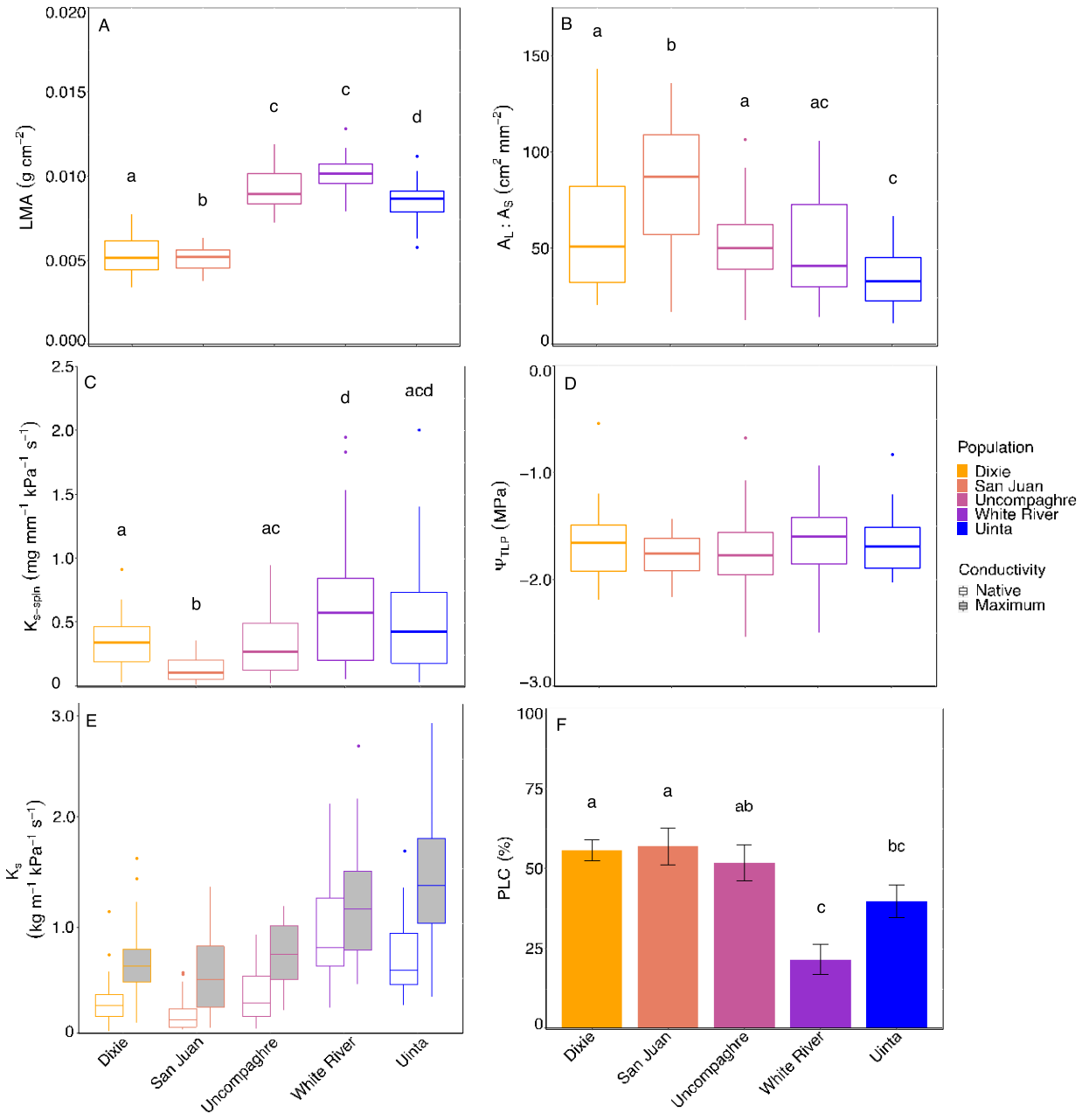

Figure 2. Measurements taken during the severe drought of 2020 showed that aspen trees from the hotter/drier populations (Dixie and San Juan) had thinner leaves, more leaf area, and xylem that was more vulnerable to drought. Measurements include: leaf mass per area (**A**, LMA), the ratio of leaf area to sapwood area (**B**, A_L:A_S), hydraulic conductivity after a cavitation-inducing pressure of -2.5 MPa (**C**, $K_{s\text{-}spin}$), leaf water potential at turgor loss point (**D**, Ψ_{TLP}), native and maximum (before and after embolism removal, respectively) hydraulic conductivity (**E**, K_s), and percent loss of conductance (**F**, PLC). Boxplots (A-E) represent median values (center bar),

990 interquartile ranges (IQR, box edges), values at most 1.5*IQR from box edge (error bars), and
991 outlying points (circular points). Bars (F) represent mean PLC and error bars represent one
992 standard error. Significant results have unique letters while nonsignificant results share the same
993 letters. Statistical results have been omitted from E to aid in visual interpretation.
994

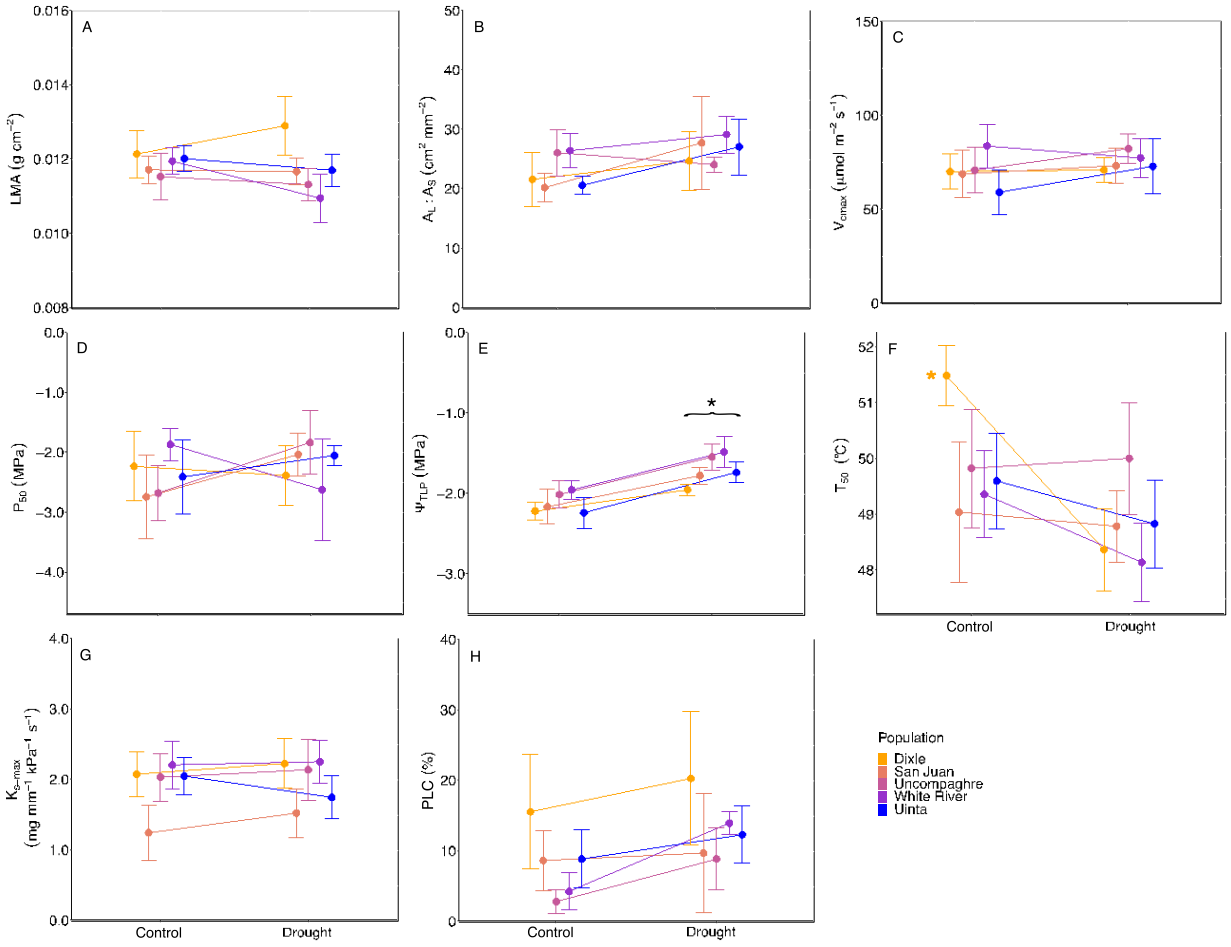

Figure 3. Measurements taken in the common garden at the end of the drought treatment showed low within-species and between-treatment differences. Leaf water potential at the turgor loss point (Ψ_{TLP}) was significant less negative in propagules that received the drought treatment, and the Dixie propagules had a significant reduction in temperature that caused 50% damage to photosystem II (T_{50}) under the drought treatment. Measurements include: leaf mass per area (**A**, LMA), the ratio of leaf area to sapwood area (**B**, A_L:A_S), maximum rate of carboxylation (**C**, V_{cmax}), pressure at which 50% loss of hydraulic conductivity occurs (**D**, P_{50}), Ψ_{TLP} (**E**), T_{50} (**F**), maximum hydraulic conductivity (**G**, $K_{s\text{-}max}$), and percent loss of conductance (**H**, PLC). Points represent mean values and error bars represent one standard error. The asterisks indicate statically significant differences where $p<0.05$. The black asterisk indicates a treatment-level significant result, and the yellow asterisk indicates a population-level significant result.

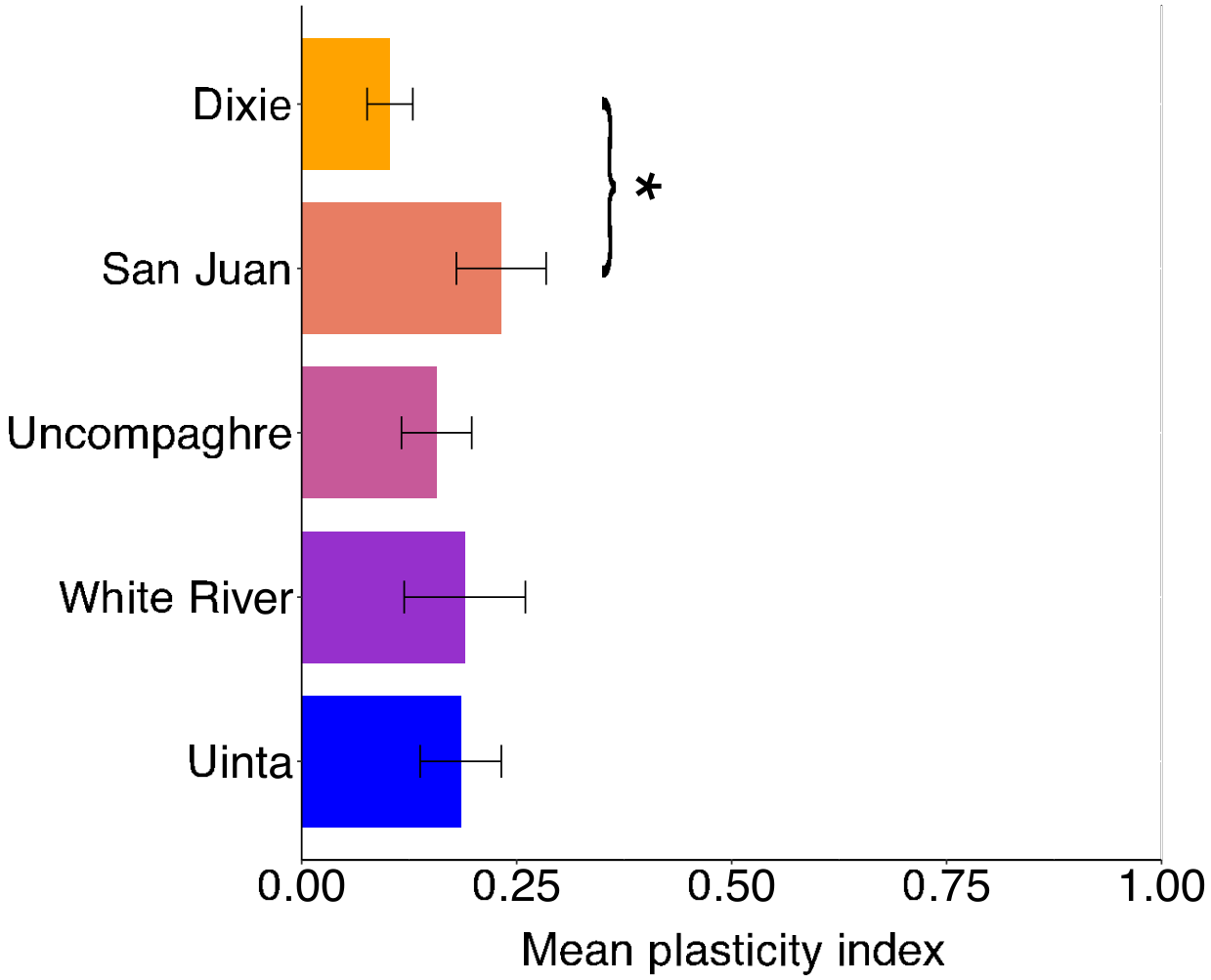

Figure 4. Average plasticity indexes for each population (determined by averageing across all growth and trait plasticity indexes as shown in Fig. S4). Bars represent mean plasticity index and error bars represent one standard error. The asterisk indicates a significant difference between propagules that originated from the Dixie and San Juan National Forests ($p < 0.05$).

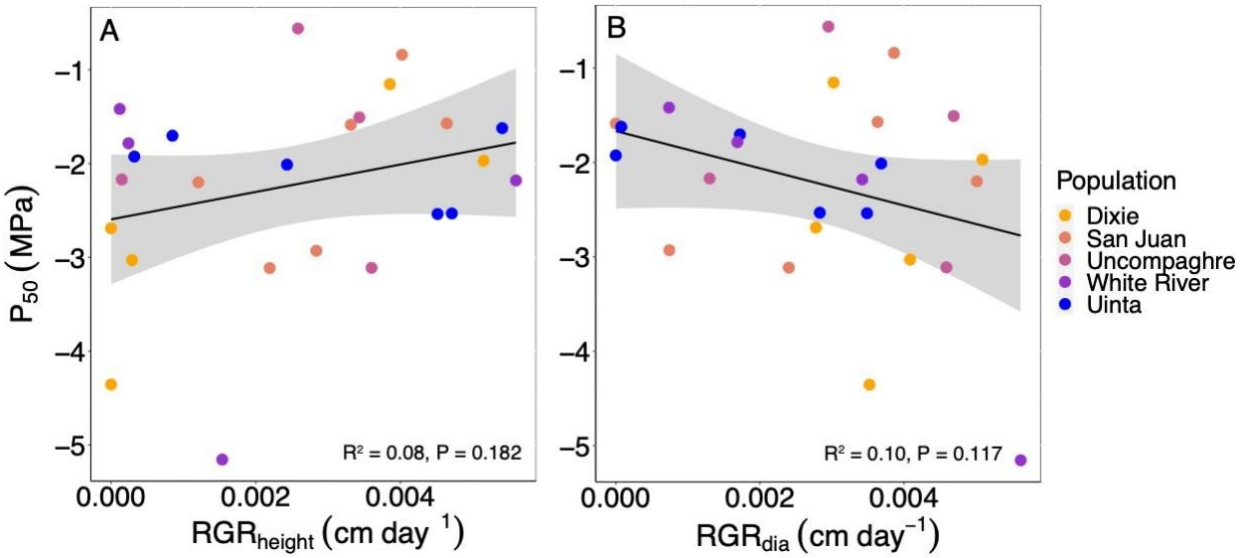

Figure 5. Among the propagules that received a drought treatment in the common garden, there was no significant trade-off between growth under wet conditions and survival under drought conditions as indicated by the linear relationship between relative growth rate in height (**A**, RGR_{height}) or diameter (**B**, RGR_{dia}) prior to the drought treatment and the pressure at which 50% loss of hydraulic conductivity occurred (P_{50}) at the end of the drought treatment. Points represent individual propagules that are colored according to the population (National Forest) of origin. The black line represents a linear model regression fit (the coefficient of determination (R^2) and p-value from the model are provided) and the grey shading represents a 95% confidence interval.

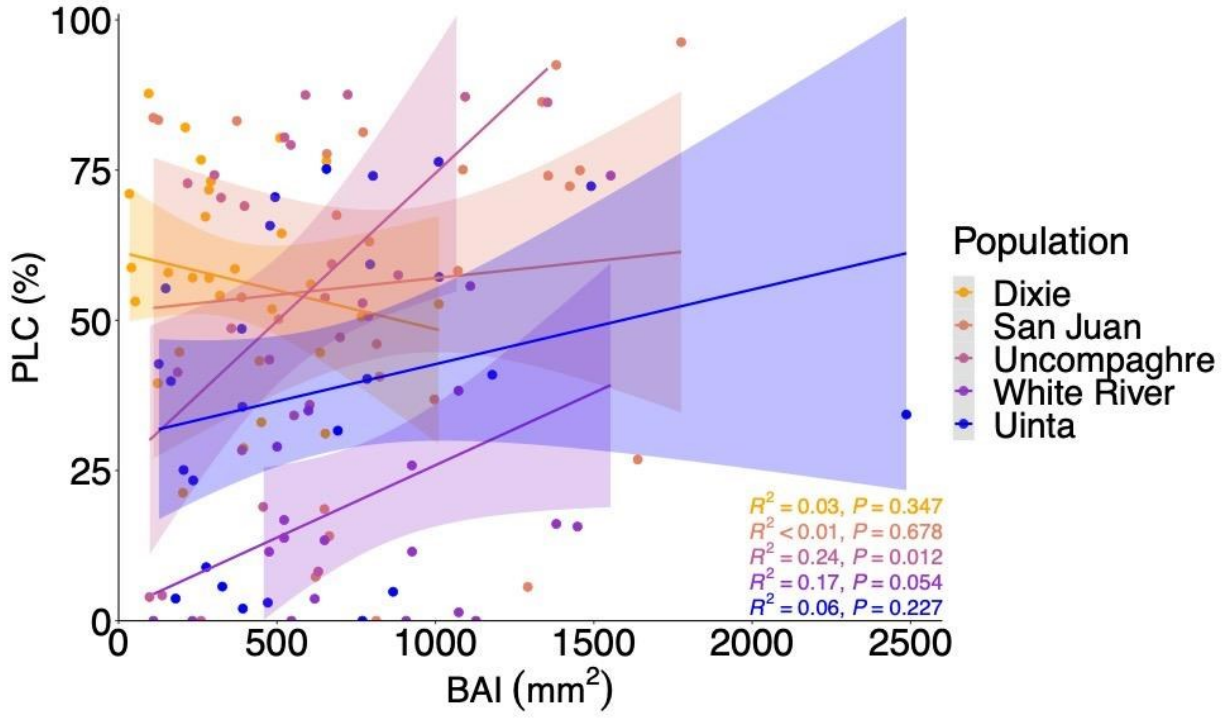

Figure 6. Among the natural populations, we observed growth-stress tolerance trade-offs in the Uncompaghre (R^2=0.24, p=0.012) and White River (R^2=0.17, p=0.054) National Forests where aspen with more growth (higher basal area increments, BAI) during wet periods (1980-1999) had xylem that was more vulnerable to the 2020 severe drought (higher percent loss of conductance, PLC). Points represent individual trees that are colored according to the population (National Forest). The lines represent linear model regression fits (coefficients of determination (R^2), and p-values models model are provided on each figure) which are also colored according to the population. 95% confidence intervals have been omitted to aid in visual interpretation.

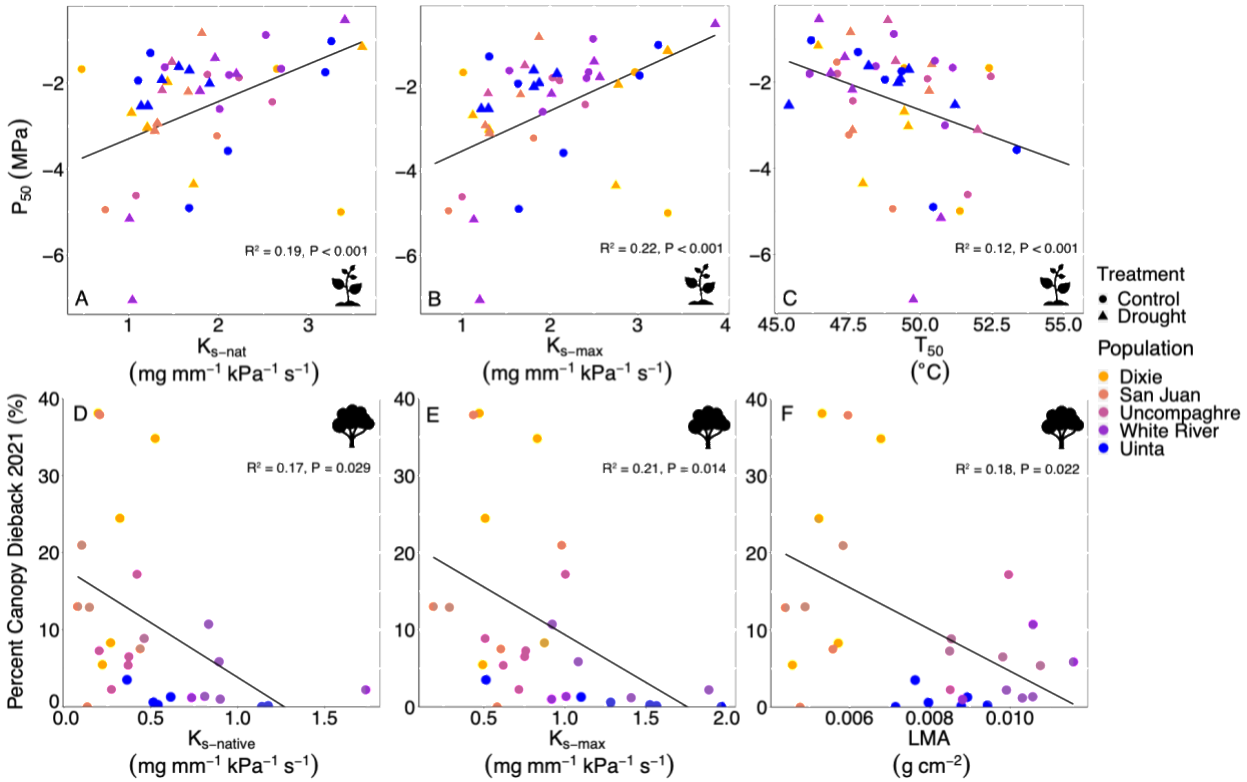

Figure 7. Trait-mediated trade-offs related to increased drought resistance occurred in both the common garden and natural populations. In the common garden, propagules with less negative pressures at which 50% loss of hydraulic conductivity occurred (P_{50}) had higher native (**A**, $K_{s\text{-}nat}$) and maximum (**B**, $K_{s\text{-}max}$) hydraulic conductivity (i.e., more drought-vulnerable xylem). Propagules with more negative P_{50} also tolerated higher temperatures before 50% damage to photosystem II occurred (**C**, T_{50}). In the natural populations, aspen trees with lower native (**D**, $K_{s\text{-}nat}$) and maximum (**E**, $K_{s\text{-}max}$) hydraulic conductivity, and lower leaf mass per area (**F**, LMA) during the severe drought of 2020 experienced heightened canopy dieback (mortality) in 2021. Points in A-C represent individual propagules, while points in D-F represent plot-level averages. Black lines represent linear model regression fits (coefficients of determination (R^2), and p-values models model are provided on each figure). Grey shading represents 95% confidence intervals. The seedling and tree icons indicate if the results occurred in the common garden or natural populations, respectively.